ChemPubSoc Europe

DOI: 10.1002/batt.201900109

BATTERIES & SUPERCAPS
Articles

Hybrid Thermo-Electrochemical In Situ Instrumentation for Lithium-Ion Energy Storage

Tazdin Amietszajew,*[a] Joe Fleming,[a] Alexander J. Roberts,[a] Widanalage D. Widanage,[b] David Greenwood,[b] Matt D. R. Kok,[c] Martin Pham,[c] Dan J. L. Brett,[c] Paul R. Shearing,[c] and Rohit Bhagat[a]

Current "state-of-the-art" monitoring and control techniques for lithium-ion cells rely on full-cell potential measurement and occasional surface temperature measurements. However, Li-ion cells are complex multi-layer devices and as such these techniques have poor resolution, limiting applicability. In this work we develop hybrid thermo-electrochemical sensing arrays placed within the cell. The arrays are integrated into A5 pouch cells during manufacture and are used to create thermal maps in parallel with anode and cathode electrochemical data. The sensor array can be adapted to a range of cell formats and chemistries and installed into commercial or other industrially relevant cells, incorporating enhanced thermal and electrochemical diagnostic capability into a standard cell build.

1. Introduction

Lithium-ion cells are seeing increased utilisation in portable electronics,[1] electric vehicles[2] and grid storage.[3] This is due to a number of advantages over alternative technologies, such as high energy and power density, low self-discharge, high output voltage and limited memory effects.[4–8] However, the market expectations and consumer demands go further requiring better performance. For example, improving performance of lithium batteries in electric vehicles (which utilise many high energy cells) might result in reducing weight, reduced charging times or improving range. Such cells can also suffer from Joule heating from internal resistances[9] resulting in excessive heat generation. Therefore, thermal management is key to preventing rapid aging or catastrophic failures via thermal runaway.[10] Furthermore, high internal cell resistances can lead to increased overpotential when charging the cells, which can drive the anode and cathode potentials outside of their respective safe operating windows. This in turn can result in electrolyte decomposition[11,12] on the cathode or lithium metal plating on the anode, which may grow in the form of dendrites and eventually pierce the separator causing an internal short circuit.[13] Here we mitigate these challenges through use of thermal and electrochemical sensor arrays placed directly into the cells.

Although some attempts were made in this direction, in previous literature the studies fail to address the impact of the sensors on the stability of the electrochemical system. *In-situ* application of thermocouples has been explored[14–22] – however such systems are limited to measuring relative temperature changes and thus require a cold junction and analogue conditioning circuits to compensate for their poor sensitivity. Reference electrode incorporation was also attempted,[23–30] however the methodologies developed were not representative of real-world applications as significant post-production modification[29] or even permanent opening of the cell[24] was required, significantly altering the electrochemical system under evaluation.[11]

Previously we have successfully deployed fibre optics technology[31] and flexible substrate thermistors[32] to monitor the cell's internal temperature, as well as standalone reference electrodes.[33] Using these sensors fast-charging was investigated and a five-fold reduction in commercial cell charging times was achieved.[34] The integration techniques were also proven to have no observable effect on the cells long-term performance. In this paper we present a further advancement in the Li-ion cells sensing technology, enabling high-precision distributed *in-operando* monitoring of Li-ion cells.

In this work we make a significant improvement to the current state-of-the-art technology by presenting a hybrid thermo-electrochemical sensor that is integrated into a pouch cell, capable of providing real-time distributed thermal maps and per-electrode potentials. The sensing points are distributed on a substrate of microns thickness, together with an incorporated reference electrode all terminating in a single standard connector. This minimises the modification to the cell's geometry while enabling a wide range of monitoring capabilities. The methodology developed here was evaluated

[a] Dr. T. Amietszajew, J. Fleming, Dr. A. J. Roberts, Prof. R. Bhagat
Coventry University
Coventry CV1 5FB (UK)
E-mail: Taz.Amietszajew@coventry.ac.uk
[b] Dr. W. D. Widanage, Prof. D. Greenwood
WMG, University of Warwick
Coventry CV4 7AL (UK)
[c] Dr. M. D. R. Kok, M. Pham, Prof. D. J. L. Brett, Prof. P. R. Shearing
Electrochemistry Innovation Lab
University College London, London WC1E 6BT (UK)

Supporting information for this article is available on the WWW under https://doi.org/10.1002/batt.201900109

for commercial manufacture using an industrially representative pouch cell scale-up line, proving its industrial viability.

Access to internal cell thermodynamics data is of significant importance to industry, especially in large scale applications, such as electric vehicles. This is due to safety and performance needs such as charge balancing and faulty module detection. The state of a battery is characterised via metrics such as State-of-Charge (SoC) and State-of-Health (SoH), however until now, no technology for direct measuring of the SoC or SoH of commercial lithium-ion batteries has been available. The electrode potentials, rather than the full-cell potential, as well as internal cell temperature profiles is what is required as a feedback signal to control the charging current and enforce efficient power limitations on the battery. Doing so will result in prolongation of the cells lifespan, e.g. by preventing lithium plating and promote highly optimised fast charging algorithms.

Measurement of individual electrode potentials and internal temperature distribution also presents a compelling opportunity for electrochemical and thermal models development. Prevailing challenges of established electrochemical models, such as the P2D model, are related to the model parameterisation for performance and degradation prediction.[35] The availability of the electrode potentials can facilitate quantifying both the thermodynamic and kinetic (solid phase diffusion) properties of the positive and negative electrodes while in a full cell format. This work subsequently mitigates the present need of preparing separate half-cell or three electrode coin cells to determine the Open Circuit Voltage or apparent diffusion coefficients of the electrodes. Such preparation activities, so far unavoidable in an effort to determine electrochemical properties, can often lead to parameters variation due to the change in cell format and scale or the differing operating conditions for the electrode materials in half-cells. Instrumented full cells will yield far more representative values of the model parameters expected in the final application.

The sensing technology described in this article can be readily applied to a range of cell formats and chemistries, offering a real-time view of the internal cell thermodynamics, assisting modelling, power mapping and monitoring under real-life use scenarios. This allows for detailed assessment of real thermal and electrochemical cell performance and safety limitations, without altering its functionality. Our approach, which enables the monitoring of the true battery state, paves the way for a deeper understanding of the Li-ion cells internal processes, permitting improvements in the existing battery technology as well as facilitating future innovation in cells design and battery systems management.

Experimental Section

Temperature and Reference Electrode Sensor Assembly

Sensor fabrication was made using standard flexible printed circuit boards manufacturing technology, using a 25 μm flexible Kapton© substrate – a material already present in most Li-ion cells and compatible with the harsh cell chemical environment. Distributed thermal sensing was made available by using low-profile (0.2× 0.3 mm) raw Surface Mount Device (SMD) Negative Temperature Coefficient (NTC) thermistors. Such devices show high precision, near linear beta curve, temperature range of −20°C to 120°C[36] and wide availability enhancing its commercial applicability. The selected thermistor elements were arranged in 6 locations on the substrate.

To enable simultaneous electrochemical measurements, an additional 2 mm diameter copper pad was located on the substrate. Most importantly, the reference electrode element of the sensor assembly is completed *in-situ* – after the cell formation a minimal amount of lithium was transferred from the cell onto the aforementioned copper pad by applying external current. The amount of lithium used constitutes less than 0.01% of the overall cell capacity, a result of the reference pad miniaturisation, and therefore has negligible impact on the cell performance. This novel approach minimised the disturbance of the sensor insertion step on the cell assembly procedure and completely eliminated the issue of handling active lithium metal in a production environment. The resulting sensor allows for parallel thermal and electrochemical monitoring, using a single flat cable connector.

To ensure the long-term stability of the assembly, a 1 μm conformal coating of Parylene was deposited on the sensors prior to embedding into the pouch cells. Parylene is a polymer with excellent mechanical and chemical stability, commonly used for its barrier properties and a highly conformal coating. Its barrier properties are known and used by other researchers.[37,38] To avoid coating of live elements – connectors, copper pads – a layer of masking tape was applied in relevant places before the coating procedure. The complete sensor assembly is shown in Figure 1.

Instrumented Cells Production

The cells considered in this study are Li-ion 1 Ah rated capacity pouch cells with Nickel-Cobalt-Aluminium (NCA) cathodes and graphite anodes. The smart-cells were built following standard industrial production procedures to evaluate real-world feasibility of our sensor embedding methodology. The complete procedure was performed using a pilot production line facility, located in a dry room with a dew-point of −45 °C to mirror an industrial setting.

To enable the instrumented cell capabilities, sensor assemblies were embedded by inserting the sensor matrix into the dry pouches immediately before electrolyte filling. The cells were then injected with commercial electrolyte mix (EC:EMC 3:7 + 1% VC, *soulbrain MI*®), vacuum-sealed and left to soak for 24 h at ambient temperature. Once the assembly process was complete, cells were subjected to a formation procedure.[39] This first cycle activates the cell materials and leads to the Solid-Electrolyte-Interface (SEI) evolution, critical for long term stability of the electrodes. This is usually performed at a low C-rate – here at C/20, although it varies with cell manufacturers and cell designs. Figure 1 outlines the instrumented-cells' build procedure.

Tomography

Cell internal structure was assessed post sensor implementation using X-ray Computed Tomography (X-ray CT). An instrumented pouch cell was imaged under compression using a Nikon XT H 225 instrument (Nikon Metrology, Tring, UK) operating with a source voltage of 175 kV at 130 μA, utilizing a 100 μm copper filter. A total of 2799 projections of 1 s exposure were obtained, recorded through 360 degrees. The X-ray transmission images were reconstructed using a proprietary reconstruction algorithm (CT Pro

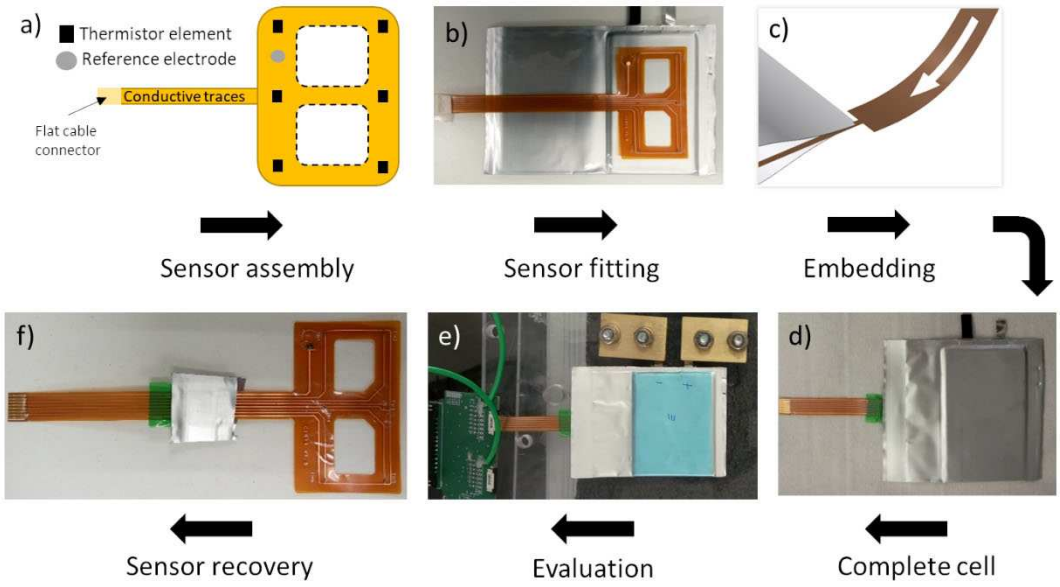

Figure 1. Smart cell assembly procedure. Sensors (a) are fitted (b) and embedded (c) in-line during the cell (d) production, enabling thermodynamic data collection (e). Flexible sensor assembly is fitted before the electrolyte injection and vacuum-sealed afterwards. The embedding procedure was found to align harmoniously with cell production, and caused no damage to the sensor (f).

Figure 2. Instrumented cell reconstructed X-ray CT image. Half of the sensor assembly is shown, fitting accurately in the middle of the electrode stack. No damage to the electrodes or the sensor was observed.

3D, Nikon Metrology). The final reconstructed volume had a voxel size of 43.8 μm. The resulting image is shown in Figure 2.

Cell Cycling and Data Collection

To evaluate the instrumented-cells behaviour during a typical operation, standard test cycles consisting of constant-current (CC) followed by constant-voltage (CV) charge and constant-current (CC) discharge were performed. Cells were cycled between 2.5 V (0% SoC) and 4.2 V (100% SoC) with a VMP3 multi-channel potentiostat (Bio-Logic Science Instruments®) using a maximum current of 400 mA. Advanced abusive case studies were also evaluated – a short-circuit event as well as overcharge cases at different current rates were investigated, showing the wide applicability of the sensors developed.

For interrogating the thermistor elements a 14-bit analogue to digital converter PicoLog (Pico®) was used. Reference electrode readings were collected using the aforementioned multi-channel potentiostat. All cell cycling was conducted in an environmental chamber maintaining an ambient temperature of 25 °C.

2. Results and Discussion

There are three aspects to the results obtained in this work. First, we analyse the feasibility of embedding functional sensors arrays into Li-ion pouch cells. Secondly follows analysis of the *in-operando* thermal and electrochemical data obtained via the embedded sensors. Finally, the advancement possibilities in battery modelling enabled by our cell instrumentation technology is discussed.

2.1. Instrumented Cells Development

A key aspect determining the usability of any type of *in-situ* sensors for energy storage is that they do not impact the system under evaluation, nor are affected by it in a detrimental way. It was found that the applied Parylene layer was a sufficient protection enabling stable readings throughout the cycling and testing conducted. The coating provided a pinhole-free conformal layer capable of preventing corrosion without creating thermal barriers, ensuring bilateral chemical neutrality. Long-term stability of embedded assemblies was evaluated in our previous work.[32]

Sensor alignment and its mechanical impact on an instrumented pouch cell has been analysed using X–CT imaging, as shown in Figure 2. The sensor array was successfully placed in equidistance to the edges of the cell – the central placement of the sensing assembly guarantees representative temperature values are obtained, key for detecting thermal non-uniformities and hot-spots. Un-obstructed ionic contact with the reference electrode, secured by its fixed position on the sensor substrate and central assembly placement, allows for proper functioning of this element. Finally, no

mechanical damage to the electrode stack was observed, further confirmed by proper functioning of the instrumented cells.

The reference electrode element provides a secondary, electrochemical sensing capability to the assembly enabling anode and cathode potential monitoring. The usually invasive nature of reference electrode insertion[30] often risks damaging the cell or changing its performance characteristics. Herein we minimised the impact by implanting the reference electrode onto an existing sensor matrix, removing the need for a separate element to be inserted into the cell. The reference electrode terminal was also integrated into the single connector alongside thermistors, further reducing the complexity of the system.

The reference electrode was completed *in-situ* by depositing lithium post integration of the sensing assembly into the pouch cell. This methodology guarantees no foreign metal contamination[40] and simplifies sensor handling and implementation significantly. Figure 3 shows the reference electrode activation and the anode and cathode electrode potential readings enabled as a result. Of notable improvement over the currently used technology[24,33,41–44] is that no metallic lithium has to be handled outside of the cell, significantly enhancing the commercial feasibility of the solution proposed.

As can be seen in Figure 3, an insignificant amount of lithium, equal to 0.01% of the overall cell capacity, was required for this process. The technological advancement offered by our solution also lies in minimising the complexity of the assembly by utilising the existing substrate with thermistors array for the added electrochemical functionality. This mitigates the implementation intricacy of a multi-component sensing array and the subsequent impact it would have on instrumented cells. This combined thermo-electrochemical monitoring capability can be used for the evaluation of the cell and to enhance the quality of parameters derived for cell modelling aspect, as discussed in the next section.

2.2. Thermal Cell Monitoring via Embedded Sensors

Surface plots in Figure 4 show the internal temperature distribution readings obtained with the embedded thermistors. The data collected is interpolated to create comprehensive thermal maps – the colour of each plot segment is established by interpolating the colourmap index value across the plot surface. Resulting are figures enabling instant analysis and easy hot-spot detection.

The temperature readings and the resulting thermal maps, shown in Figure 4, can detect minute heterogeneities in temperature distribution. Such phenomena can be observed even at comparatively[34,45] low cycling rate of 400 mA (C/2.5) using a single cell. Complete discharge-charge cycle is displayed in Video 1, where it can be observed that most heat is generated towards the end of the discharge phase rather than during charge, after which the cell quickly recovers. This can vary widely depending on the cell chemistry, geometry and cycling profiles.[46]

To prevent overheat and catastrophic events,[10] the commonly agreed safe temperature limit for the widely available Li-ion cells is set at approximately 60 °C.[47–49] However,

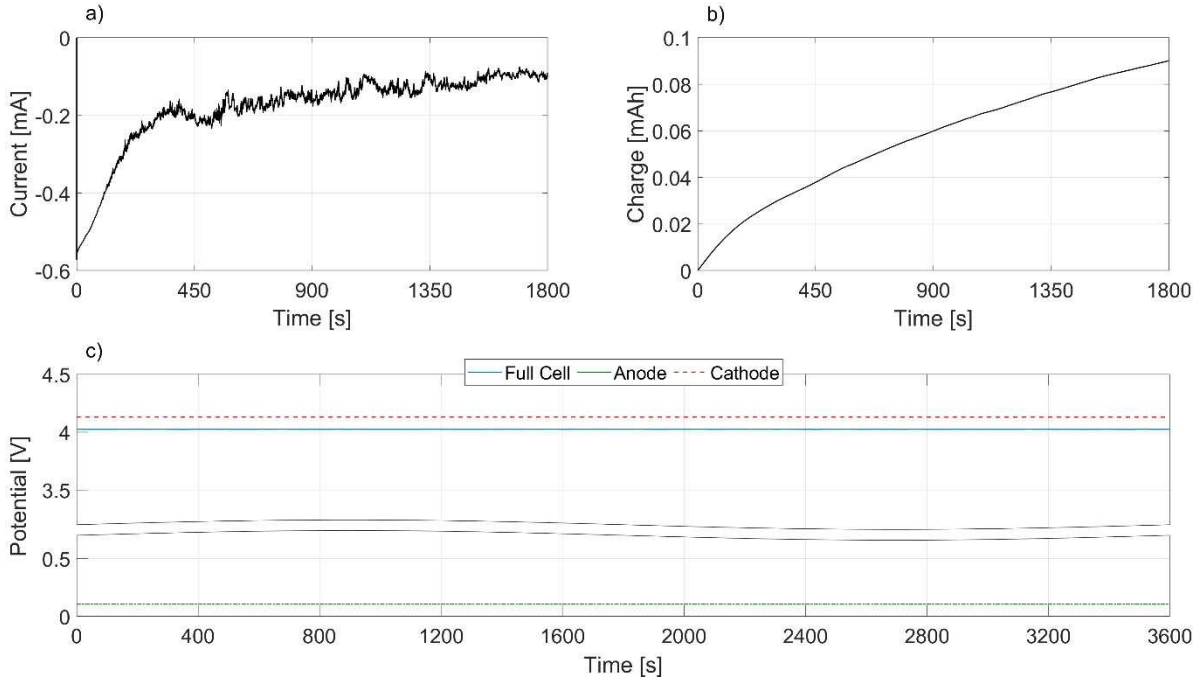

Figure 3. Activation of the reference electrode. Low current was passed over 30 min (a) resulting in a charge of 900 μAh (b). This subsequently activated the reference electrode, enabling stable per-electrode potential monitoring (c). This approach has negligible impact on the overall cell capacity while removing the challenge of handling metallic lithium outside of the cell during assembly, significantly enhancing the real-life industrial applicability.

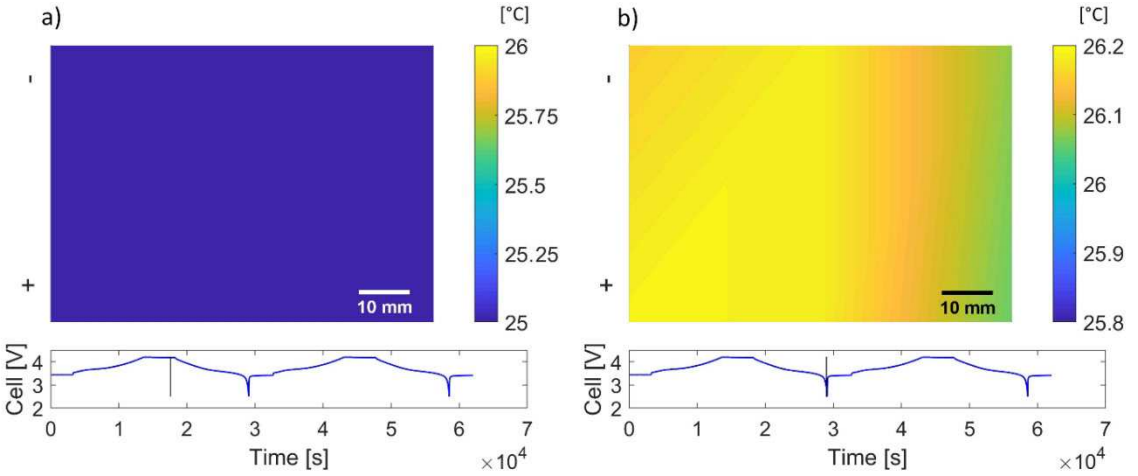

Figure 4. Internal thermal maps obtained from the embedded sensors, respectively, showing a) rest phase and b) end of discharge. Cells were cycled at a rate of C/2.5, yet even at such low C-rate a temperature gradient is identifiable with the *in-situ* sensors. Corresponding cycling profile points are indicated with black bars on the voltage curves underneath each panel. Real-time representation of the charge-discharge cycles with the thermal and voltage responses mapped is available as Video 1 in the Supporting Information.

not all of the cell has to reach a runaway temperature to cause a chain reaction – localised heat zones, potentially leading to thermal runaways, have to be eliminated and continuously monitored to ensure the safety and longevity of the device in use. This is especially pronounced in high performance systems[10,31,50] and currently dictates extensive testing[46,51–53] before battery deployment. The proposed distributed thermal monitoring solution offers an easily applicable, high-sensitivity and low-impact alternative that can be used across the design, optimisation and real-life use stages. This is a significant improvement over the currently used technology, where thermal sensors are only attached to the accessible surface of a selected sample of cells within the module or pack,[22] which within a battery module can lead to failure to identify hot-spots and temperature variations.[51] This added capability has the potential to support the Battery Management System in addressing the performance[19,33,34,54] and safety concerns.[55]

2.3. Electrochemical Cell Monitoring via Embedded Sensors

Cell voltage profiles for both anode and cathode (relative to lithium) as well as standard full-cell voltage readings are shown in Figure 5. Monitoring of these parameters was performed

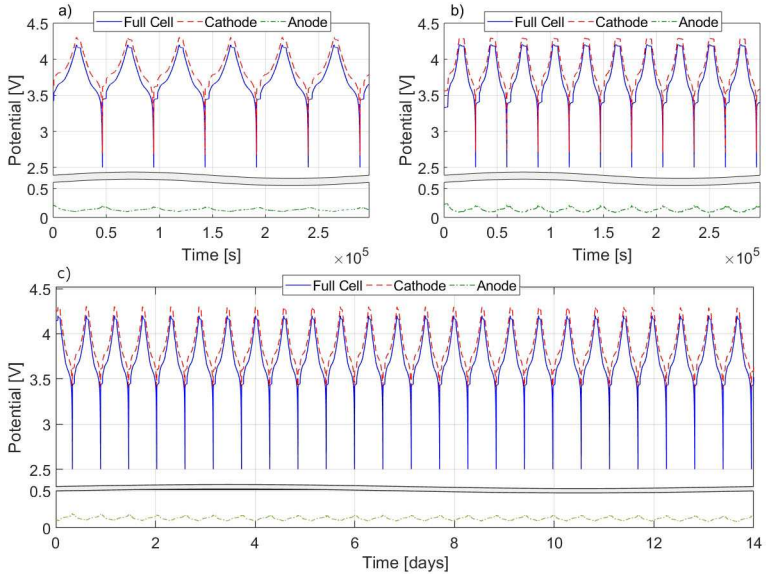

Figure 5. Anode, cathode and full cell potential profiles of a smart-cell fitted with hybrid sensors. Panel a) represents 200 mA (C/5) cycling rate and panel b) is double that at 400 mA. It can be instantly seen that the anode and cathode responses differ when a higher current is applied to the cell, resulting in more pronounced voltage peaks. The reference electrode element was subsequently monitored over the course of 2 weeks, providing stable readings as shown in (c).

using the same sensor assembly used for thermal mapping. The tests were conducted over several days, the results showing the reference electrode provide stable and repeatable readings.

The stability of the readings obtained confirms the functionality of the reference electrode element. It is evident that the flat reference electrode miniature pad achieves sufficient ionic contact with the rest of the cell, while at the same time it is not adding to the extent of the cell modification and minimises the risk of internal short circuiting otherwise present when introducing additional wires. This is a significant advancement over the previously reported cell instrumentation methodology.[30,33,56] Most importantly, the proposed solution of simultaneously enabling both thermal and electrochemical sensing capabilities has been successfully integrated into a standard full-cell pouch manufacturing process.

Together with the *in-situ* thermal monitoring, tracing of the per-electrode parameters – enabled by the co-implemented reference electrode – is key to understanding the operational limitations of Li-ion cells. Continuous monitoring of the anode and cathode potentials alongside distributed thermal profiling allows us to closely observe and avoid exceeding stability limits,[34,56–59] subsequently enabling power mapping and increasing the safety of the system in real-life applications. Specifically – cell health monitoring algorithms,[60,61] usually developed based on a total cell voltage, can now be adapted and applied to the individual electrode potentials. Doing so can reduce the degradation of cells by avoiding lithium plating, reduce SEI growth rate[62] and promote significantly optimised rapid charging algorithms[34] – the advances and impact on battery modelling and control algorithm development will be the focus of our studies following this paper.

Internal thermal maps obtained via the embedded sensors, respectively a) rest phase and b) end of discharge. Cells were cycled at a rate of C/2.5, yet even at such low C-rate a temperature gradient is identifiable with the *in-situ* sensors.

Internal thermal maps obtained via the embedded sensors, respectively a) rest phase and b) end of discharge. Cells were cycled at a rate of C/2.5, yet even at such low C-rate a temperature gradient is identifiable with the *in-situ* sensors.

3. Conclusions

The objective of this study was to develop a widely applicable sensing methodology enabling significantly improved insight into the internal Li-ion cell thermodynamics, capable of assisting power mapping and in operando thermodynamic monitoring. The method proposed herein allows detailed assessment of real-time thermal and electrochemical cell performance and safety limitations, without altering its functionality. This offers significant benefits over the industry standard of monitoring cell performance using thermocouple sensors attached to the skin and a full-cell voltage and from those inferring core parameters. This work shows how implementing distributed flexible thermo-electrochemical *in-situ* sensors is an enhanced method for performance characterisation and verification of Li-ion cells' state.

Most importantly, as the manufacturing of current-generation lithium-reference electrodes requires highly specialised equipment, specialist training, know-how and knowledge – this cannot be readily industrialised. Here, reference electrodes are implemented onto the same substrate as thermal sensors and are completed whilst inside the cell, using minuscule amounts of lithium from the cells' electrochemical system. This mitigates the need for handling highly reactive alkali metals and complicating the cell assembly process, while enabling the highly beneficial reference electrode capability.

Due to the flexibility of the sensing elements layout, these sensors can be developed to fit multiple cell types of various dimensions, offering wide compatibility. The concept was validated by successful assembly of the instrumented cells in a pilot line battery production facility, enabling the *in-operando* thermal and electrochemical sensing capabilities in a classic pouch cell format. This demonstrated the manufacturing feasibility of the proposed solution in a semi-industrial setting. Subsequent X–CT analysis confirmed the electrode stack was left intact by the centrally-aligned sensor array, allowing for proper functioning of the cells.

High fidelity thermal data obtained with instrumented cells can be used to produce thermal maps, offering visual indication of heat-zones and enhancing our understanding of the cell heat-generation characteristics. This, together with the electrochemical measurements represents a vital source of information, critical to refining the State-of-Charge and State-of-Health metrics. SoC and SoH algorithms, so far developed based on a total cell voltage, can now be adapted and applied to the individual electrode potentials. Thereby SoC and SoH can be resolved attributed to the separate electrode, offering sub-cell resolution of the charge and aging parameters.

Refinement of these metrics to cell components will consequently result in a unique opportunity to devise advanced Battery Management System algorithms in future BMS releases, as well as aid in new cells design and validation. The advances and impact on battery modelling and control algorithm development will be the next round of studies following this paper. In summary, the hybrid thermo-electrochemical *in-situ* sensing methodology proposed here has the potential to drive innovation in both performance and operational safety mapping, as well as thermodynamic modelling and management of the energy storage systems.

Data Statement

The datasets generated and analysed during the described study are available from the corresponding author on a reasonable request.

Acknowledgments

Correspondence and requests for materials should be addresses to the corresponding author. T.A., J.F., A.J.R., M.D.R.K and M.P. performed the experiments and analysed the data. R.B. and D.G. supervised the project and offered guidance. All authors designed the experiments and wrote the manuscript. This research was done with support from EPSRC for project TRENDS (reference number EP/R020973/1) and M-RHEX (reference number EP/R023581/1).

Conflict of Interest

The authors declare no conflict of interest.

Keywords: electrochemistry · energy storage · in situ instrumentation · lithium ion batteries · sensors

[1] M. Bini, D. Capsoni, S. Ferrari, E. Quartarone, P. Mustarelli, *Rechargeable Lithium Batteries*, Elsevier Ltd., **2015**.
[2] L. Gaines, R. Cuenca, *Costs of Lithium-Ion Batteries for Vehicles*, Argonne, IL, **2000**.
[3] C. for E. Cooperation, *Environmentally Sound Management of End-of-Life Batteries from Electric-Drive Vehicles in North America*, **2015**.
[4] C. J. Bae, A. Manandhar, P. Kiesel, A. Raghavan, *Energy Technol.* **2016**, *4, 851-855*, DOI 10.1002/ente.201500514.
[5] A. Opitz, P. Badami, L. Shen, K. Vignarooban, A. M. Kannan, *Renewable Sustainable Energy Rev.* **2017**, *68*, 685–692.
[6] B. Nykvist, M. Nilsson, *Nat. Clim. Change* **2015**, *5*, 329–332.
[7] P. Miller, *Johnson Matthey Technol. Rev.* **2015**, *59*, 4–13.
[8] B. Scrosati, J. Garche, *J. Power Sources* **2010**, *195*, 2419–2430.
[9] P. V. Braun, J. Cho, J. H. Pikul, W. P. King, H. Zhang, *Curr. Opin. Solid State Mater. Sci.* **2012**, *16*, 186–198.
[10] Q. Wang, P. Ping, X. Zhao, G. Chu, J. Sun, C. Chen, *J. Power Sources* **2012**, *208*, 210–224.
[11] A. Lex-Balducci, W. Henderson, P. Stefaon, in *Lithium-Ion Batter. Adv. Mater. Technol.*, **2012**, pp. 149–196.
[12] J. Xia, K. J. Nelson, Z. Lu, J. R. Dahn, *J. Power Sources* **2016**, *329*, 387–397.
[13] D. Deng, *Energy Sci. Eng.* **2015**, *3*, 385–418.
[14] N. S. Spinner, K. M. Hinnant, R. Mazurick, A. Brandon, S. L. Rose-pehrsson, S. G. Tuttle, *J. Power Sources* **2016**, *312*, 1–11.
[15] P. J. Osswald, S. V Erhard, J. Wilhelm, H. E. Hoster, A. Jossen, *J. Electrochem. Soc.* **2015**, *162*, A2099–A2105.
[16] T. Waldmann, M. Wohlfahrt-Mehrens, *ECS Electrochem. Lett.* **2015**, *4*, A1–A3.
[17] G. Zhang, L. Cao, S. Ge, C. Y. Wang, C. E. Shaffer, C. D. Rahn, *J. Electrochem. Soc.* **2014**, *161*, A1499–A1507.
[18] C. Forgez, D. Vinh Do, G. Friedrich, M. Morcrette, C. Delacourt, *J. Power Sources* **2010**, *195*, 2961–2968.
[19] T. Waldmann, G. Bisle, B. I. Hogg, S. Stumpp, M. A. Danzer, M. Kasper, P. Axmann, M. Wohlfahrt-Mehrens, *J. Electrochem. Soc.* **2015**, *162*, A921–A927.
[20] N. Martiny, A. Rheinfeld, J. Geder, Y. Wang, W. Kraus, A. Jossen, *IEEE Sens. J.* **2014**, *14*, 3377–3384.
[21] M. S. K. Mutyala, J. Zhao, J. Li, H. Pan, C. Yuan, X. Li, *J. Power Sources* **2014**, *260*, 43–49.
[22] N. Martiny, A. Rheinfeld, J. Geder, Y. Wang, W. Kraus, A. Jossen, in *IEEE Sens. J.*, (1)TUM CREATE (2)Institute for Technical Electronics, Technical University of Munich (3)Institute for Electrical Energy Storage Technology, Technical University of Munich, **2014**, pp. 3377–3384.
[23] W. Fang, O. J. Kwon, C. Y. Wang, *Int. J. Energy Res.* **2010**, *34*, 107–115.
[24] P. Liu, J. Wang, J. Hicks-Garner, E. Sherman, S. Soukiazian, M. Verbrugge, H. Tataria, J. Musser, P. Finamore, *J. Electrochem. Soc.* **2010**, *157*, A499.
[25] Y. Zhang, C.-Y. Wang, *J. Electrochem. Soc.* **2009**, *156*, A527–A535.
[26] G. Nagasubramanian, D. H. Doughty, *J. Power Sources* **2005**, *150*, 182–186.
[27] Q. Wu, W. Lu, J. Prakash, *J. Power Sources* **2000**, *88*, 237–242.
[28] J. R. Belt, D. M. Bernardi, V. Utgikar, *J. Electrochem. Soc.* **2014**, *161*, A1116–A1126.
[29] G. Nagasubramanian, *J. Power Sources* **2000**, *87*, 226–229.
[30] E. McTurk, C. R. Birkl, M. R. Roberts, D. A. Howey, P. G. Bruce, *ECS Electrochem. Lett.* **2015**, *4*, DOI 10.1149/2.0081512eel.
[31] J. Fleming, T. Amietszajew, E. McTurk, D. Greenwood, R. Bhagat, G. Dave, R. Bhagat, E. McTurk, D. Greenwood, R. Bhagat, *HardwareX* **2018**, *3*, 100–109.
[32] J. Fleming, T. Amietszajew, J. Charmet, A. J. Roberts, D. Greenwood, R. Bhagat, *J. Energy Storage* **2019**, *22*, 36–43.
[33] E. McTurk, T. Amietszajew, J. Fleming, R. Bhagat, *J. Power Sources* **2018**, *379*, 309–316.
[34] T. Amietszajew, E. McTurk, J. Fleming, R. Bhagat, *Electrochim. Acta* **2018**, *263*, 346–352.
[35] M. Doyle, T. F. Fuller, J. Newman, *J. Electrochem. Soc.* **1993**, *140*, 1526–1533.
[36] "NCP03WF104F05RL Specifications," **2018**.
[37] W. Li, D. C. Rodger, E. Meng, J. D. Weiland, M. S. Humayun, Y. C. Tai, *Proc. 2006 Int. Conf. Microtechnologies Med. Biol.* **2006**, 105–108.
[38] J. Charmet, J. Bitterli, O. Sereda, M. Liley, P. Renaud, H. Keppner, *J. Microelectromech. Syst.* **2013**, *22*, 855–864.
[39] Y. Masaki, R. J. Brodd, A. Kozawa, *Lithium-Ion Batteries*, Springer, New York, **2009**.
[40] A. Lewenstam, F. Scholz, *Handbook of Reference Electrodes*, Springer Berlin Heidelberg, Berlin, Heidelberg, **2013**.
[41] B. Markovsky, A. Rodkin, Y. . Cohen, O. Palchik, E. Levi, D. Aurbach, H.-J. Kim, M. Schmidt, *J. Power Sources* **2003**, *119*, 504–510.
[42] J. C. Burns, L. J. Krause, D.-B. Le, L. D. Jensen, A. J. Smith, D. Xiong, J. R. Dahn, *J. Electrochem. Soc.* **2011**, *158*, A1417–A1422.
[43] Z. Chu, X. Feng, L. Lu, J. Li, X. Han, M. Ouyang, *Appl. Energy* **2017**, *204, 1240-1250*, DOI 10.1016/j.apenergy.2017.03.111.
[44] P. Keil, S. F. Schuster, J. Wilhelm, J. Travi, A. Hauser, R. C. Karl, A. Jossen, *J. Electrochem. Soc.* **2016**, *163*, A1872–A1880.
[45] P. Keil, A. Jossen, *J. Energy Storage* **2016**, *6*, 125–141.
[46] S. Goutam, J. M. Timmermans, N. Omar, P. Van den Bossche, J. Van Mierlo, *Energies* **2015**, *8*, 8175–8192.
[47] M. Dubarry, B. Y. Liaw, M.-S. Chen, S.-S. Chyan, K.-C. Han, W.-T. Sie, S.-H. Wu, *J. Power Sources* **2011**, *196*, 3420–3425.
[48] A. Väyrynen, J. Salminen, *J. Chem. Thermodyn.* **2012**, *46*, 80–85.
[49] S. Al-Thyabat, T. Nakamura, E. Shibata, A. Iizuka, *Miner. Eng.* **2013**, *45*, 4–17.
[50] G. J. Offer, V. Yufit, D. A. Howey, B. Wu, N. P. Brandon, *J. Power Sources* **2012**, *206*, 383–392.
[51] L. H. Saw, Y. Ye, A. A. O. Tay, W. T. Chong, S. H. Kuan, M. C. Yew, *Appl. Energy* **2016**, *177*, 783–792.
[52] P. Cicconi, D. Landi, M. Germani, *Appl. Energy* **2017**, *192*, 159–177.
[53] A. Pesaran, *Adv. Automot. Batter. Conf.* **2001**, 10.
[54] P. Bohn, G. Liebig, L. Komsiyska, G. Wittstock, *J. Power Sources* **2016**, *313*, 30–36.
[55] S. Panchal, I. Dincer, M. Agelin-Chaab, R. Fraser, M. Fowler, *Appl. Therm. Eng.* **2016**, *96*, 190–199.
[56] R. Raccichini, M. Amores, G. Hinds, *Batteries* **2019**, *5*, 12.
[57] B. Vortmann-Westhoven, M. Winter, S. Nowak, *J. Power Sources* **2017**, *346*, 63–70.
[58] K. Uddin, S. Perera, W. Widanage, L. Somerville, J. Marco, *Batteries* **2016**, *2*, 13.
[59] C. R. Birkl, M. R. Roberts, E. Mcturk, P. G. Bruce, D. A. Howey, *J. Power Sources* **2016**, *341*, 1–35.
[60] M. Dubarry, N. Qin, P. Brooker, *Curr. Opin. Electrochem.* **2018**, *9*, 106–113.
[61] M. Dubarry, B. Y. Liaw, *J. Power Sources* **2009**, *194*, 541–549.
[62] J. Christensen, J. Newman, *J. Electrochem. Soc.* **2004**, *151*, A1977–A1988.

Manuscript received: April 6, 2019
Revised manuscript received: August 15, 2019
Version of record online: September 3, 2019